Cell Death and Differentiation (2015) 22, 476–487

www.nature.com/cdd

Lysosomal membrane permeabilization and autophagy blockade contribute to photoreceptor cell death in a mouse model of retinitis pigmentosa

N Rodríguez-Muela[1,3], AM Hernández-Pinto[2,3], A Serrano-Puebla[1,3], L García-Ledo[1], SH Latorre[1], EJ de la Rosa[2] and P Boya*[,1]

Retinitis pigmentosa is a group of hereditary retinal dystrophies that normally result in photoreceptor cell death and vision loss both in animal models and in affected patients. The rd10 mouse, which carries a missense mutation in the *Pde6b* gene, has been used to characterize the underlying pathophysiology and develop therapies for this devastating and incurable disease. Here we show that increased photoreceptor cell death in the rd10 mouse retina is associated with calcium overload and calpain activation, both of which are observed before the appearance of signs of cell degeneration. These changes are accompanied by an increase in the activity of the lysosomal protease cathepsin B in the cytoplasm of photoreceptor cells, and a reduced colocalization of cathepsin B with lysosomal markers, suggesting that lysosomal membrane permeabilization occurs before the peak of cell death. Moreover, expression of the autophagosomal marker LC3-II (lipidated form of LC3) is reduced and autophagy flux is blocked in rd10 retinas before the onset of photoreceptor cell death. Interestingly, we found that cell death is increased by the induction of autophagy with rapamycin and inhibited by calpain and cathepsin inhibitors, both *ex vivo* and *in vivo*. Taken together, these data suggest that calpain-mediated lysosomal membrane permeabilization underlies the lysosomal dysfunction and downregulation of autophagy associated with photoreceptor cell death.
Cell Death and Differentiation (2015) **22,** 476–487; doi:10.1038/cdd.2014.203; published online 12 December 2014

Autophagy is a cellular self-degradative pathway that mediates the recycling of damaged or disposable cell components and is activated in situations of nutritional, oxidative and other forms of stress.[1] This process begins with the formation of the autophagosome, an intracellular double-membrane organelle that surrounds parts of the cytoplasm containing organelles and protein aggregates. Autophagosomes subsequently fuse with lysosomes to initiate the degradation of the engulfed cellular components. Autophagy dysfunction has been implicated in many pathological conditions including infections, cancer and muscular and degenerative diseases.[2] In the nervous system, autophagy has a key role in preventing intracellular accumulation of misfolded and/or aggregated proteins, and its pharmacological upregulation through the administration of rapamycin and other drugs exerts protective effects against a wide range of proteinopathies.[3] Moreover, defects in different stages of the autophagy pathway, including autophagosome formation, cargo recognition and lysosomal fusion and degradation, have been often implicated in neurodegeneration.[4]

In addition to their degradative role, lysosomes are emerging as key regulators of cellular homeostasis, acting as nutritional sensors or actively participating in cell death.[5–7] Lysosomal alterations including increases in lysosomal pH and lysosomal membrane permeabilization (LMP) have been demonstrated in Alzheimer's and Parkinson's diseases,[8,9] and mutations in lysosomal enzymes cause defects in autophagy, inducing a marked neurodegenerative phenotype in patients with lysosomal storage disorders.[10] LMP induces the selective translocation of cathepsins to the cytoplasm, triggering caspase-dependent and -independent cell death.[11–13] LMP has been implicated in mammary gland involution in physiological conditions,[14] indicating that lysosomal-mediated cell death is not merely a consequence of accidental lysosomal damage. As *in vivo* administration of cathepsin inhibitors attenuates cell death in this model, a similar approach could hold therapeutic potential for the treatment of diseases associated with LMP, including Parkinson's disease, Niemann–Pick disease type A and stroke.[7,10,15] Oxidative stress and calpain activation are some of the many stimuli that can induce LMP, and have been observed both *in vitro* and *in vivo*.[7] Several pathological processes in the nervous system associated with cell death, including excitotoxicity and ischaemia–reperfusion, have been linked to increased calpain activation.[16] Calpains have also been shown to cleave many intracellular substrates including autophagy and lysosomal proteins,[17,18] suggesting links between calcium levels, calpain activation, lysosomal damage and autophagy blockade.

Recent findings have begun to shed light on the role of autophagy in the retina. We previously reported decreased

[1]Autophagy Lab, Department of Cellular and Molecular Biology, Centro de Investigaciones Biológicas, CSIC, Ramiro de Maetzu 9, Madrid 28040, Spain and [2]3D Lab, Department of Cellular and Molecular Medicine, Centro de Investigaciones Biológicas, CSIC, Ramiro de Maetzu 9, Madrid 28040, Spain
*Corresponding author: P Boya, Autophagy Lab, Department of Cellular and Molecular Biology, Centro de Investigaciones Biológicas, CSIC, Ramiro de Maetzu 9, Madrid 28040, Spain. Tel: +34 91 8373112; Fax: +34 91 5360432; E-mail: patricia.boya@csic.es
[3]Shared authorship.
Abbreviations: DHE, dihydroethidium; LMP, lysosomal membrane permeabilization; P, postnatal day; PBS, phosphate-buffered saline; TUNEL, terminal deoxynucleotidyl transferase-mediated dUTP nick-end labelling; Wt, wild type
Received 14.7.14; revised 04.11.14; accepted 05.11.14; Edited by M Piacentini; published online 12.12.14

autophagy flux in the retinas of aged mice,[19] and demonstrated photoreceptor cell death and decreased dim-light vision in the neuronal-specific Atg5-deficient mouse, a phenotype that closely resembles that observed during physiological aging.[19] We have also demonstrated the essential cytoprotective role of autophagy *in vivo* in response to retinal ganglion cell damage in experimental models of glaucoma.[20] A recent study described lysosomal basification and decreased autophagic flux in travecular meshwork cells in response to chronic oxidative stress, with important implications for the pathogenesis of glaucoma.[21] Furthermore, specific Atg5 deletion in pigment epithelium leads to reduced levels of visual pigments and vision alterations,[22] indicating that autophagy has an important role in sustaining retinal pigment epithelium function.

Retinitis pigmentosa is a large group of genetic disorders that normally involves photoreceptor cell death and leads to vision loss in both animal models and affected patients. To date, no treatment for this devastating disease has been developed to clinic. The study of animal models is thus essential to unravel the mechanisms of photoreceptor degeneration involved in these disorders and to identify therapeutic targets. The rd10 mouse, which harbours a mutation in the rod-specific phosphodiesterase gene *Pde6b*, is a suitable model of human retinitis pigmentosa.[23,24] This mutation results in reduced enzymatic function leading to increased cGMP and rod cell death, peaking around postnatal day 25 (P25), with only residual vision remaining after P30.[24,25] Here we show that rd10 mice exhibit massive intracellular calcium accumulation and m-calpain (calpain-2) activation at early ages, before the peak of photoreceptor cell death, that correlate with the blockade of autophagic flux. Moreover, we demonstrate an increase in cathepsin B activity in the cytoplasm of rd10 photoreceptors that correlates with the activation of DNAse II-dependent cell death. Induced calcium overload in wild-type (Wt) retinal explants phenocopies the degenerative features seen in rd10 retinas: lysosomal damage, cathepsin translocation and cell death. Finally, we show that calpain and cathepsin inhibitors attenuate cell death both *in vitro*, *ex vivo* and *in vivo.* Taken together, these data suggest that calpain-mediated LMP underlies the lysosomal dysfunction and downregulation of autophagy associated with photoreceptor cell death.

Results

Autophagy blockade is observed in rd10 retinas before the onset of other neurodegenerative features. Cell death peaks in the rd10 mouse around P25.[24,25] As autophagy is one of the major intracellular stress responses, we analysed the lipidation of the autophagosomal marker LC3 in Wt and rd10 retinas at different stages. Days before the peak of cell death, at P20, levels of the lipidated form of LC3 (LC3-II) were decreased in rd10 *versus* Wt mice, whereas those of the autophagy substrate p62 were increased (Figure 1a). These alterations were also detected at later stages (P30 and P60), suggesting that autophagy is blocked in rd10 retinas before and during the degenerative process. Moreover, this autophagy blockade was correlated with marked activation of mTOR, as evidenced by an increase in the phosphorylation of its substrate P-S6. We next investigated whether the reduced lipidation of LC3 resulted in alterations in autophagy flux in rd10 retinas. Retinal explants were incubated in the absence or presence of lysosomal protease inhibitors (Figure 1b). A reduction in autophagy flux in rd10 *versus* Wt retinas was already evident at P16. Interestingly, these differences in autophagy flux were greater at early time points, well before the onset of cell death, suggesting that photoreceptors are the main cells contributing to autophagy in the retina. We next explored the expression of GFP-LC3 levels in the retina of rd10-GFP-LC3 animals by fluorescence analysis (Figure 1c). At P25, levels of LC3 were reduced in the photoreceptor cell layer in rd10 *versus* Wt mice. Interestingly, Ambra1, an essential regulator of autophagy, was completely absent from the photoreceptor layer in rd10 retinas (Figure 1c and Supplementary Figure 1). Taken together, these data describe several alterations in the autophagy pathway in rd10 retinas before the appearance of signs of degeneration, such as photoreceptor cell death.

Rd10 retinas exhibit calcium accumulation and increased calpain activation in the early stages of the degenerative process. Mutations in the gene encoding the rod-specific phosphodiesterase PDE6B in the rd1 mouse have been associated with oxidative stress and abnormal calcium accumulation.[26] We performed a time-course analysis of both processes in rd10 retinas using flow cytometry. Retinas from Wt and rd10 mice were dissociated and incubated with Fluo-3 and dihydroethidium (DHE) to evaluate intracellular calcium levels and oxidative stress, respectively. At P18, rd10 retinas already displayed increased calcium levels as compared with the corresponding controls (Figure 2a), whereas increases in oxidative stress were first significant at P23 (Figure 2b). At P25, increases in 8-hydroxydeoxyguanosine, a modified base produced after DNA is attacked by reactive oxygen species, were detected in rd10 retinas, accompanied by the presence of nitrosylated proteins (Figure 2c and Supplementary Figure 2), confirming the presence of oxidative damage in the later stages of retinal degeneration. As early as P15, rd10 retinas also showed signs of ER stress, as evidenced by increased levels of phosphorylated eIF2α and the glucose-regulated protein-78 (GRP78) (Figure 2d), and calpain activation (Figure 2e). These findings indicate that calcium accumulation, ER stress and calpain-2 activation are early features of rd10 retinal degeneration, occurring well before the peak of photoreceptor cell death.

Cathepsin B activity is decreased in lysosomes and increased in the cytoplasm of rd10 photoreceptors. Calpain activation has been postulated to induce LMP, translocation of cathepsin to the cytosol and cell death.[6] To explore whether the calpain activity detected in our system could also lead to LMP, we used immunofluorescence to localize cathepsin B and Lamp-1 in Wt and rd10 retinas at P20, before the peak of photoreceptor cell death. In Wt retinas, cathepsin B immunostaining frequently colocalized with the lysosomal marker Lamp-1 (Figure 3a, white arrows). By contrast, this pattern was observed less frequently in rd10

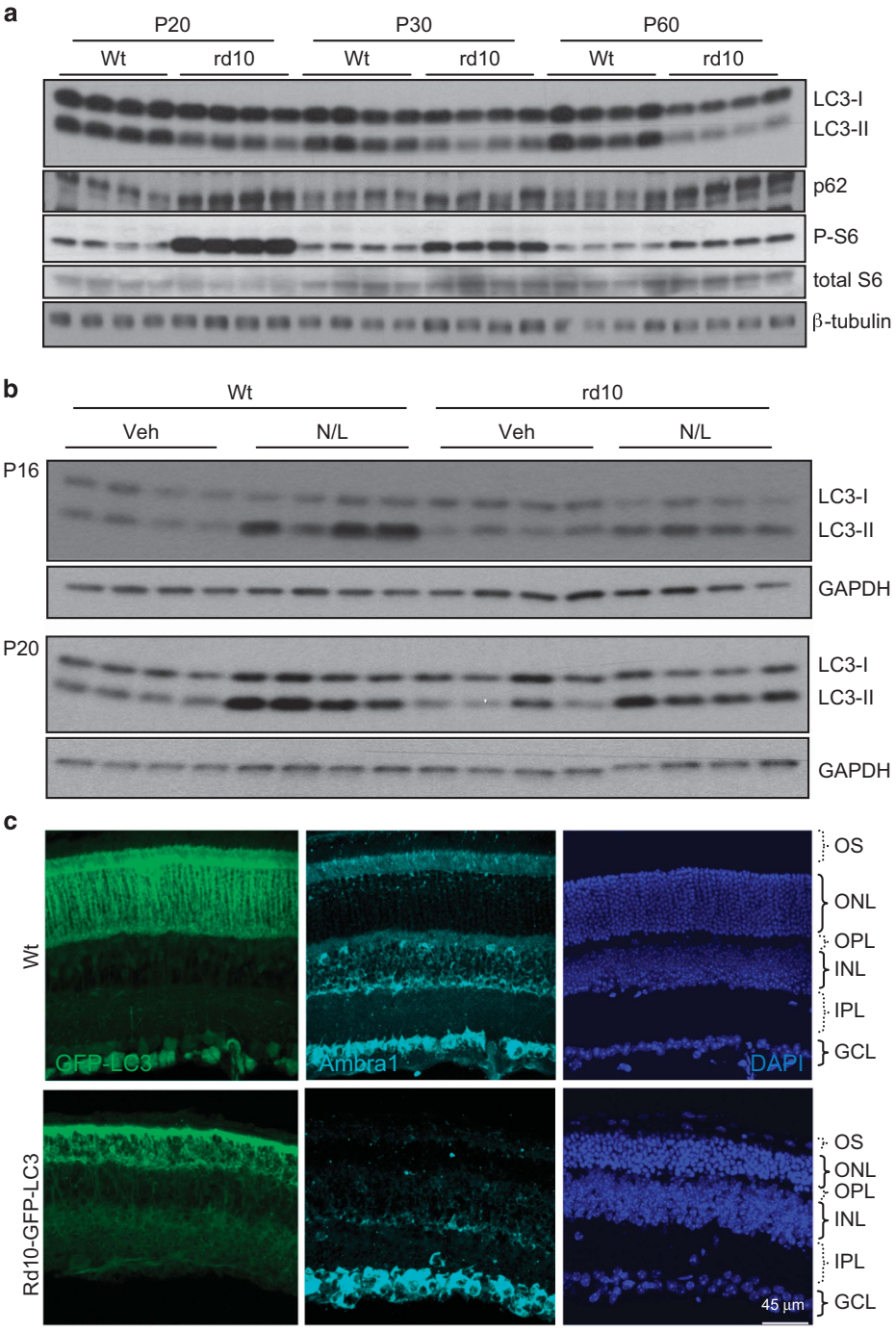

Figure 1 Autophagy and autophagic flux are reduced in rd10 retinas before the onset of neurodegeneration. (**a**) Immunoblot showing LC3, p62 and phosphorylated and total S6 in retinal lysates from Wt and rd10 retinas at the indicated ages. (**b**) Analysis of LC3 lipidation as a measure of autophagic flux in Wt and rd10 retinas incubated for 3 h with vehicle (Veh) or 20 mM ammonium chloride plus 100 μM leupeptin and leupeptine (N/L). β-Tubulin and GAPDH are used as loading controls. (**c**) Retinal cryosections from GFP-LC3 and GFP-LC3/rd10 mice at P25 stained with Ambra1 (cyan) and DAPI to visualize the nuclei (blue). Scale bar, 45 μm. GCL, ganglion cell layer; INL, inner nuclear layer; IPL, inner plexiform layer; ONL, outer nuclear layer; OPL, outer plexiform layer; OS, outer segment

retinas. We next analysed cathepsin B activity, as determined using the fluorogenic substrate Magic Red, in Wt and rd10 retinal explants. Rd10 retinas exhibited high levels of cathepsin B activity in photoreceptor cells, with a uniform diffuse staining pattern throughout the cytoplasm, suggesting cytosolic localization of the enzyme (Figure 3b and Supplementary Figure 3). These observations suggest that cathepsin B is translocated outside the lysosome, possibly pointing to LMP in rd10 retinas. Further supporting this view, we observed an increase in the activity of lysosomal enzyme DNAse II (Figure 3c), which colocalized with terminal deoxynucleotidyl transferase-mediated dUTP nick-end

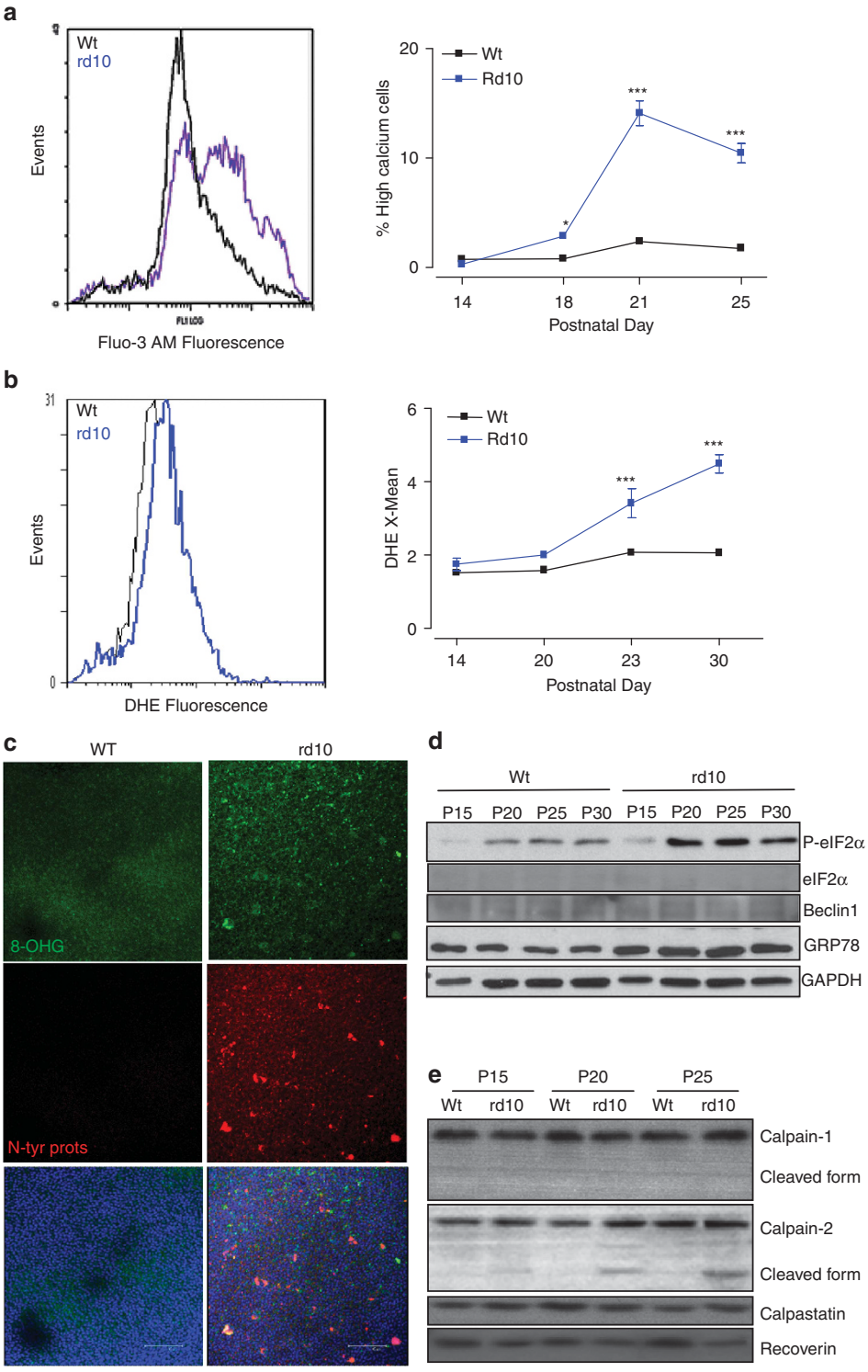

Figure 2 Rd10 retinas exhibit increased calcium levels, oxidative and ER stress and calpain activation. Determination of calcium levels by cytometry with Fluo-3AM (**a**) and of oxidative stress with DHE (**b**). Histogram shows profile of Wt and rd10 retinas at P21 for (**a**) and P23 for (**b**), and the graphs display the quantification at different ages (***$P<0.005$, $n=4$). (**c**) Immunostaining of flat-mounted retinas from Wt and rd10 mice at P25 using DAPI (blue) anti-8-hydroxydeoxyguanosine, to detect oxidative damage to DNA (green) and *S*-nitrosocysteine antibody for S-nitrosylated proteins (red). Scale bar, 45 μm. (**d**) Immunoblot of retinal lysates from Wt and rd10 retinas of the indicated ages using P-eIF2α, eIF2α and GRP78 antibodies to measure ER stress and Beclin1. (**e**) Immunoblots of retinal lysates from Wt and rd10 retinas of the indicated ages using antibodies specific for the total and cleaved forms of calpain-1, calpain-2 and calpastatin (the cleaved forms provide an indication of enzyme activation). Recoverin antibody was used as a control to ensure equal loading of photoreceptors in each sample. Images are representative of three different experiments performed in duplicate

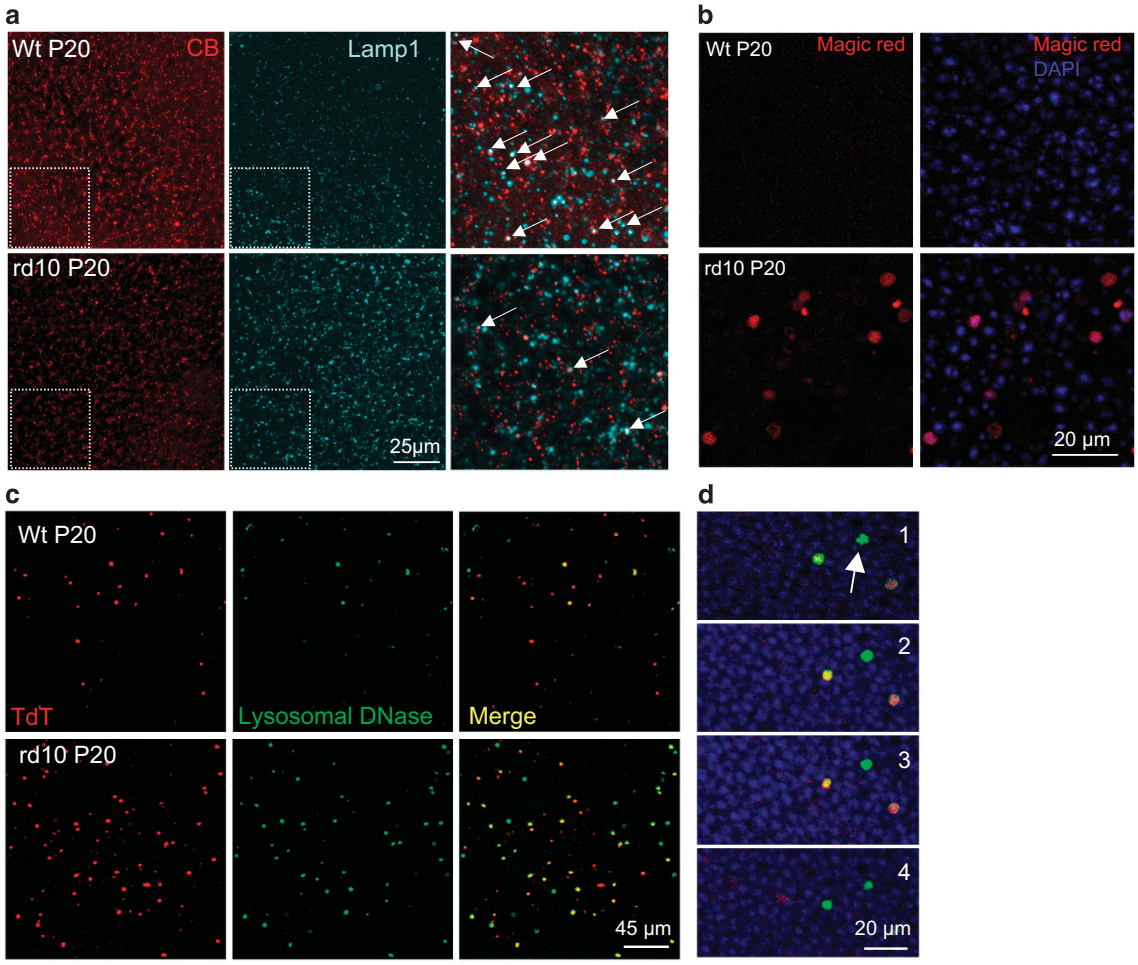

Figure 3 Rd10 retinas display LMP and increased cytoplasmic cathepsin B activity. (**a**) Immunostaining for cathepsin B (red) and Lamp-1 (cyan) in flat-mounted Wt and rd10 retinas at P20. Higher magnifications are shown in the insets and colocalization is indicated with white arrows. Scale bar, 25 μm. (**b**) Cathepsin B activity in Wt and rd10 retinas at P20 as determined using the Magic Red Cathepsin B Assay Kit (red), with and DAPI counterstaining (blue). Scale bars, as indicated. (**c**) Determination of DNase I and II activity using ApopTag ISOL Dual Fluorescence Apoptosis Detection in Wt and rd10 retinas at P20. DNase I is detected with TdT (red) and lysosomal DNase II (green), and DAPI counterstaining was performed to label the nuclei. Scale bars, as indicated. (**d**) Images of different confocal planes demonstrate that not all cells display staining for both TdT and II (white arrow)

labelling (TUNEL)-stained apoptotic cells in some cells (Figure 3d). Taken together, these data suggest that LMP in rd10 retinas leads to an increase in the activity of lysosomal enzymes that in turn induces photoreceptor cell death (Figure 3c).

Calcium overload provokes LMP and cell death in Wt retinal explants, an effect prevented by inhibitors of lysosomal proteases and autophagy. Intracellular calcium increases are observed in rd10 retinas before the appearance of signs of degeneration. To experimentally induce calcium overload, we treated Wt retinal explants with either vehicle or the calcium ionophore A23187 and assessed the effects on autophagy. Calcium ionophore treatment for 3 h increased intracellular calcium to a similar concentration to that seen in rd10 *in vivo* retinas (Figures 4a and b), and after 6 h increased the levels of oxidative stress (Figures 4c and d) and triggered photoreceptor cell death (Figures 4e and f). Interestingly, A23187 treatment also inhibited autophagy flux, as evidenced by the lack of LC3-II accumulation in retinas treated with protease inhibitors (Figure 4g).

Furthermore, A23187 treatment promoted the translocation of cathepsin B from lysosomes to the cytosol, as revealed by the decreased staining of cathepsin and the change in the pattern of Magic Red staining from discrete puncta (lysosomal) in vehicle-treated retinas to diffuse staining throughout the whole cell in the treated retinas (Supplementary Figures 4A and B). These data indicate that incubation of retinal explants with the calcium ionophore increases cytoplasmic calcium levels, attenuates autophagy flux and triggers LMP and cell death, thus recapitulating key events that occur in the degenerating rd10 retina.

As our data demonstrate that cathepsin translocation after LMP induces photoreceptor cell death in the rd10 retinas, we next treated retinal explants with A23187 in the presence or absence of cathepsin and calpain inhibitors. The marked increase in the number of TUNEL-positive cells observed after A23187 treatment of Wt retinal explants was largely prevented

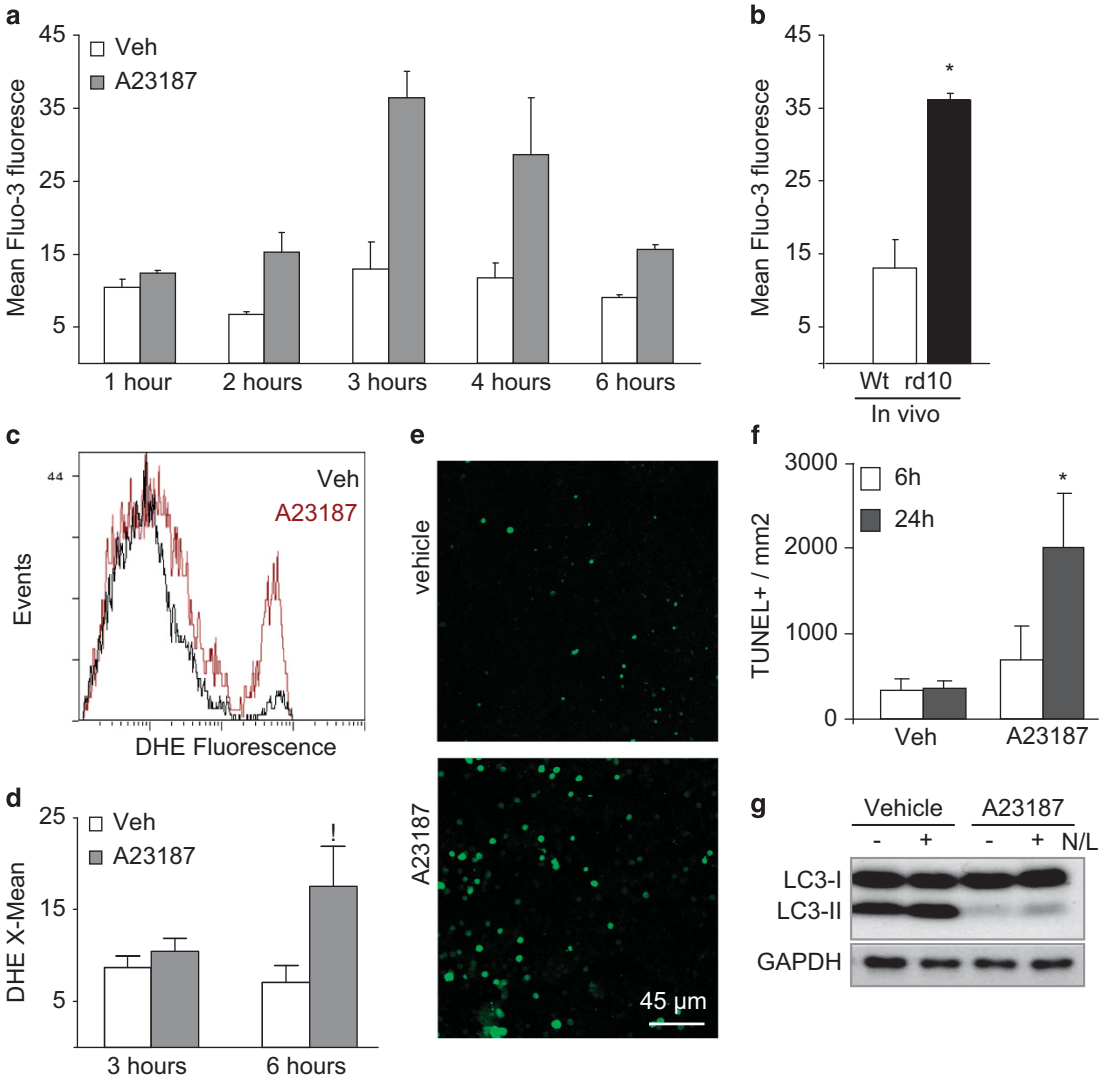

Figure 4 The rd10 phenotype can be mimicked by incubating Wt retinal explants with the calcium ionophore A23187. (**a**) Flow cytometry analysis of calcium levels using Fluo-3AM in P20 Wt retinas cultured for the indicated times with either vehicle (dimethylsulphoxide (DMSO)) or the calcium ionophore A23187 at 5 μM. Data represent mean $\pm$ S.E.M. (**b**) P20 Wt and rd10 retinas were incubated in parallel with Fluo-3AM for comparison (*$P<0.05$, $n=4$). Data represent mean $\pm$ S.E.M. (**c**) Oxidative stress determination with DHE by flow cytometry in P20 Wt retinas cultured for 6 h with either vehicle (DMSO) or the calcium ionophore A23187, and (**d**) quantification of DHE mean fluorescence at the indicated times (*$P<0.05$, $n=4$). Data represent mean $\pm$ S.E.M. (**e**) TUNEL staining of flat-mounted P20 Wt retinas treated for 24 h with vehicle or 5 μM A23187. Quantification of TUNEL-positive nuclei 6 and 24 h after treatment is shown in (**f**) (*$P<0.05$, $n=4$). Data represent mean $\pm$ S.E.M. (**g**) P20 Wt retinal lysates were incubated for 24 h with vehicle or A23187, and in the presence or absence of lysosomal inhibitors for the last 4 h of culture (N/L), and then immunoblotted for LC3

in the presence of cathepsin and calpain inhibitors (Figures 5a and b). These findings support the view that LMP induced an increased cytosolic calcium level, and leads to cathepsin-dependent cell death of photoreceptor cells. We next investigated whether autophagy modulation affected photoreceptor cell death induced by calcium overload. We treated retinal explants with A23187 in the absence or presence of rapamycin or wortmannin to induce and inhibit autophagy, respectively. Strikingly, rapamycin enhanced A23187-induced cell death, an effect that was blocked in the presence of protease inhibitors (Figures 5c and d). Conversely, autophagy blockade with wortmannin attenuated A23187-induced cell death (Figures 5c and e). In conclusion, calcium overload in Wt retinal explants phenocopies the degenerative features seen in rd10 retinas (lysosomal damage, cathepsin translocation and cell death), suggesting that, in a situation of autophagy impairment, cell death is ameliorated by the attenuation of autophagy activity, and exacerbated by autophagy stimulation.

Cathepsin inhibitors attenuate retinal degeneration in rd10 mice *in vivo*. Having determined the possible course of retinal degeneration, both *in vivo* and experimentally, we next investigated the effect of calpain and cathepsin inhibitors on cell death and photoreceptor cell loss in rd10 mice. Intravitreal administration of cathepsin and protease inhibitors in rd10 mice significantly attenuated photoreceptor cell death (Figure 6a). We next explored whether rapamycin

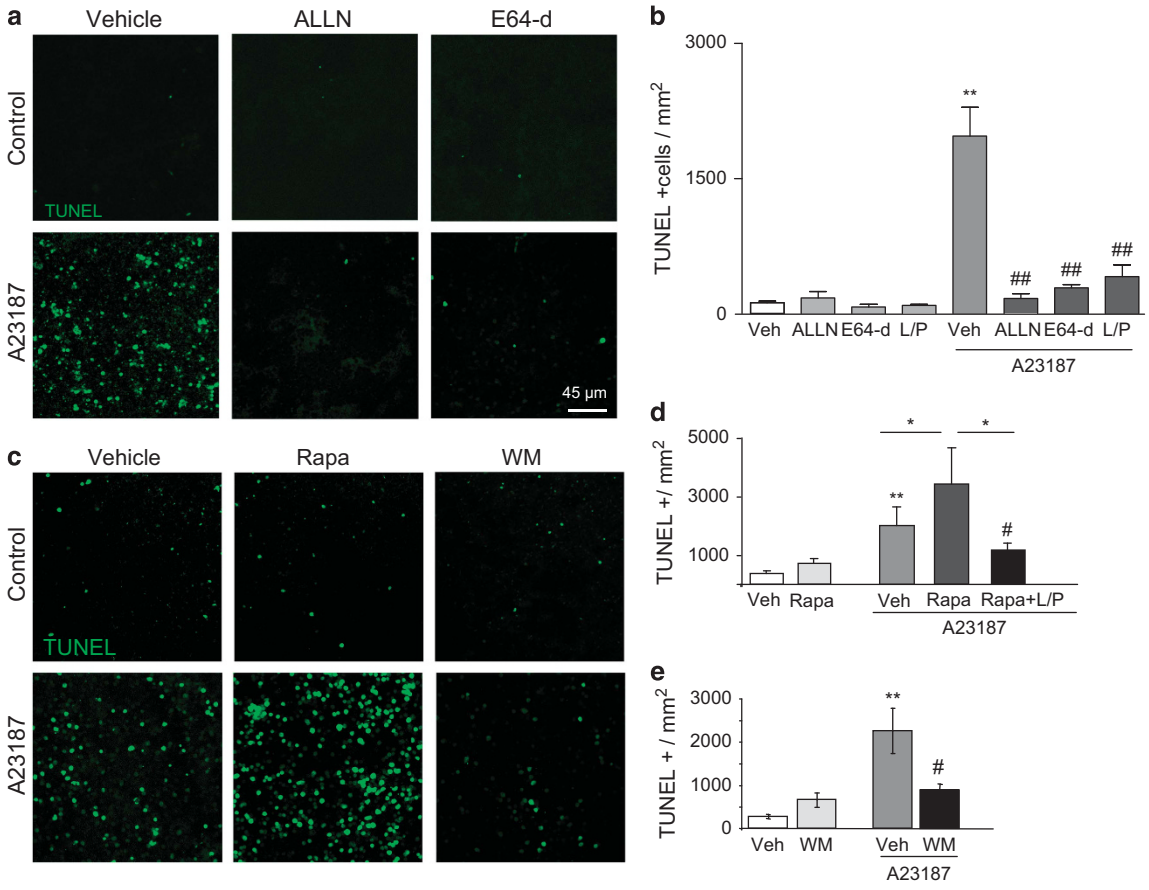

Figure 5 Calpain and cathepsin inhibitors block A23187-induced cell death in Wt retinas. (**a**) TUNEL staining in P20 Wt retinas cultured for 24 h with vehicle or A23187 in the presence or absence of calpain inhibitors (ALLN), cathepsin inhibitors (E64-d) or inhibitors of lysosomal proteases (combination of pepstatin A and leupeptin, L/P). Quantification of TUNEL-positive cells is shown in (**b**). Data represent mean ± S.E.M. (**$P<0.05$ *versus* vehicle; $^{\#\#}P<0.05$ *versus* A23187, $n=4$ for vehicle and $n=5$ for A23187-treated retinas). (**c**) TUNEL staining in P20 Wt retinas cultured for 24 h with vehicle or A23187 in the presence or absence of the autophagy inducer rapamycin or the autophagy inhibitor wortmannin. Quantification of TUNEL-positive nuclei is shown in (**d** and **e**). Data represent mean ± S.E.M. (*$P<0.05$ *versus* vehicle; $^{\#}P<0.05$ *versus* A23187, $n=8$)

was able to induce autophagy activity in *ex vivo* Wt retinas subjected to calcium overload. Indeed, autophagy was activated as determined increase levels of LC3-II and further increase in the presence of lysosomal inhibitors. More importantly, a similar effect was observed in the rd10 retinas, indicating that rapamycin is able to unregulate autophagic flux in rd10 retinas *ex vivo* (Figure 6b). As observed after the induction of calcium overload in Wt mice, intraperitoneal rapamycin treatment exacerbated cell death in rd10 mice (Figure 6c). Interestingly, *in vivo* rapamycin treatment increased the levels of calpain-2 (Figure 6d), supporting the view that upregulation of autophagy *in vivo* is detrimental when lysosomal function is impaired. To further support these data and to rule out the possibility that the inhibition of other prosurvival activities of mTOR by rapamycin, rather than the induction of autophagy, is responsible for the increased rate of cell death, we performed experiments with trehalose, an mTOR-independent inducer of autophagy.[27] As it is shown in Supplementary Figure 5, trehalose slightly increased the number of TUNEL-positive cells in the rd10 retinas and significantly increased the percentage of reduction of the outer nuclear layer thickness. Taken together, these data indicate that calcium overload in rd10 retinas induces calpain activation, LMP and cell death, and point to autophagy downregulation as a promising new therapeutic strategy to delay the degenerative process in *retinits pigmentosa* patients.

Discussion

In the present study, we demonstrate that calcium overload, both induced experimentally in Wt retinas or occurring pathophysiologically in rd10 mouse retinas, triggers calpain activation, resulting in permeabilization of the lysosomal membrane and consequent photoreceptor cell death. In both models cell death is attenuated by inhibition of calpain or cathepsin activity. Furthermore, we demonstrate that rd10 retinas show reduced lipidation of the autophagosomal marker LC3-II, lower levels of autophagy regulators and a marked reduction in autophagy flux. Interestingly, we found that stimulation of autophagy with rapamycin both *ex vivo* and *in vivo* increased cell death, while downregulation of autophagy rescued photoreceptor cell death.

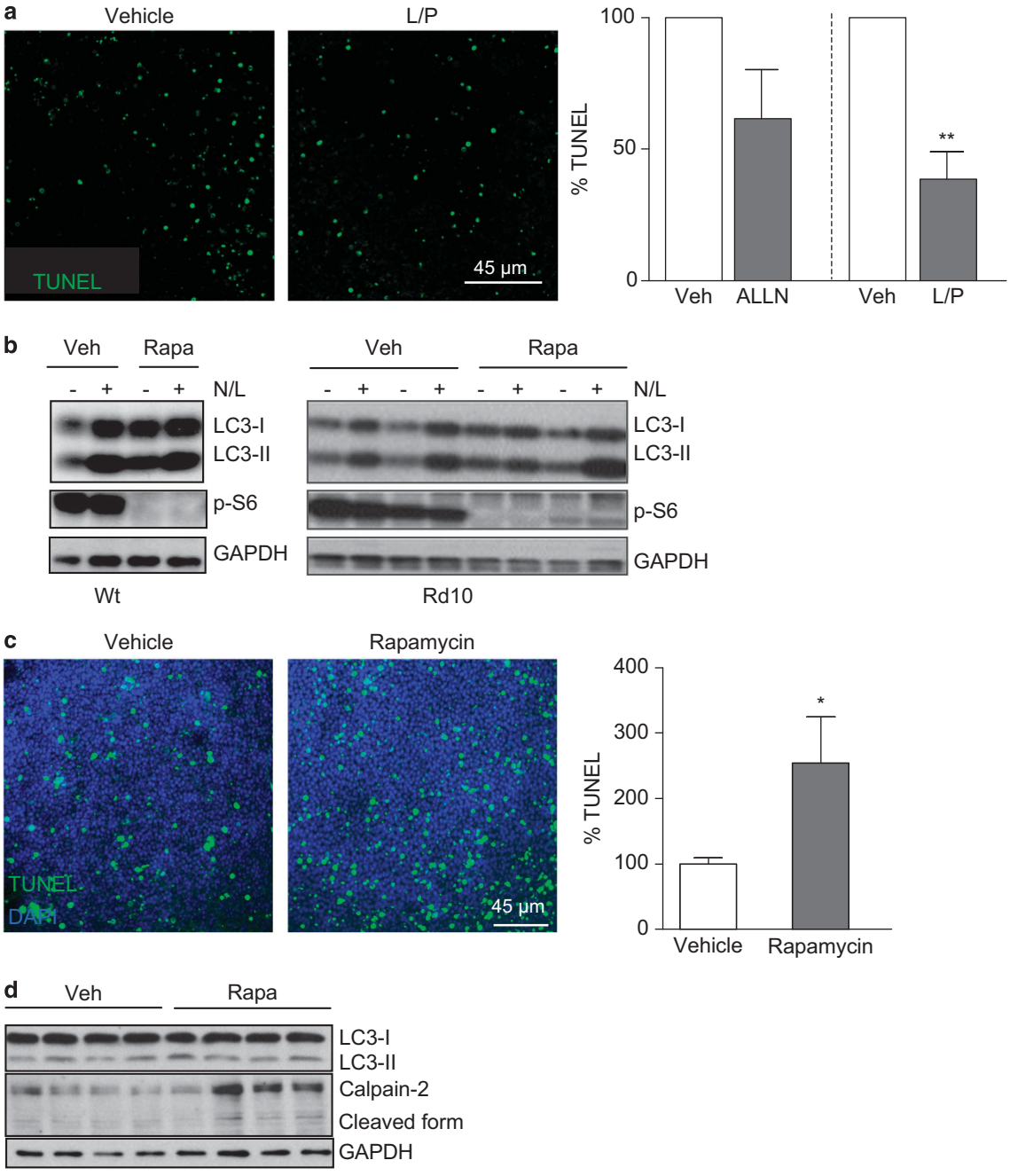

Figure 6 Cell death *in vivo* is augmented by autophagy induction and attenuated by lysosomal inhibitors. (**a**) Flat-mounted retinas showing TUNEL staining at P25 from rd10 mice that were intravitreally injected with the indicated inhibitor in one eye or its vehicle in the contralateral eye at P23. Data are presented as a percentage of each control eye, whose number of TUNEL-positive cell was considered as 100% (**$P<0.01$, $n=4$). (**b**) Western blot analysis in Wt (left) and rd10 (right) retinas cultured for 6 h with 200 nM rapamycin in the absence (−) or presence (+) of ammoniun chloride and leupeptin to block lysosomal activity. Autophagy is determined with LC3-II levels and mTOR blockage is determined by P-S6 kinase. GAPDH is used as a loading control. (**c**) TUNEL staining of flat-mounted retinas and quantification from P23 rd10 mice that received rapamycin or vehicle systemically every 2 days from P13 until the day of killing (*$P<0.05$, $n=8$). (**d**) Western blot analysis in retinas form animals treated as in (**c**) and blotted for LC3, calpain-2 and GAPDH as loading controls

An extensive literature supports a link between altered calcium signalling and neuronal death. In particular, excessively high glutamate levels in synaptic terminals leads to calcium overload, which contributes to death during brain aging and in many neurodegenerative conditions.[28] In the rd1 model of retinitis pigmentosa, abnormal calcium accumulation in photoreceptor cells has been linked to cell death independently of cGMP levels.[29] Several studies have also implicated intracellular calcium in autophagy regulation,[30] and the differing outcomes described suggest that calcium-dependent autophagy regulation may be both cell- and context-dependent.[31] Some reports indicate autophagy

activation after calcium overload, while others have described autophagy blockade before autophagosome closure in response to thapsigargin or the calcium ionophore A23187.[32,33] We found that the levels of lipidated LC3 were reduced *in vivo* both in rd10 retinas and in A23817-treated Wt retinas. Moreover, we observed a clear reduction in autophagy flux in both cases, suggesting impairment in the correct flow of autophagosome formation and degradation. Several studies indicate that calpain activation after calcium overload attenuates autophagy by cleaving specific autophagy regulators.[17,34] We found that calpain activation was increased in rd10 retinas as early as P15. In line with these findings, reduced LC3-II levels and increased calpain activation have also been described in *N*-methyl-*N*-nitrosourea (MNU)-induced photoreceptor cell death, another experimental mouse model of human retinitis pigmentosa.[35] Interestingly, in that model and in a model of photoreceptor cell death after retinal detachment,[36] cell death is prevented by calpain inhibition *in vivo*.

The autophagy regulator Ambra1 was recently proposed as a substrate for calpains in certain conditions.[37] In line with this view, we observed a marked reduction in Ambra1 levels in rd10 mouse retinas, suggesting that the protein is degraded by the activated calpains. While the activation of calpain-2 (also known as m-calpain) requires millimolar calcium concentrations, calpain-1 (μ-calpain) is activated by micromolar concentrations.[16] Our data indicate that treatment of Wt retinas for 3 h with a calcium ionophore increases the intracellular calcium concentration to a level comparable to that seen in untreated rd10 retinas. Ionophore treatment should equilibrate intra- and extracellular calcium levels, which in our culture media are in the millimolar range. We thus propose a selective role of calpain-2 in blocking autophagy flux in rd10 retinas, similar to that described in a model of ischaemia–reperfusion in the liver.[38] However, we cannot rule out the possibility that other autophagy regulators are degraded by calpains, and thus contribute to the autophagy blockade.

Lysosomal membrane stability is essential to avoid the leakage of acidic hydrolases into the cytosol and decreases in the intracellular pH that can trigger cell necrosis.[13] However, selective and partial membrane permeabilization often releases certain proteases, such as cathepsin B and D, into the cytoplasm. These enzymes, which are also active at neutral pH, trigger a cascade of controlled (inhibitable) events leading to caspase-dependent and -independent cell death[11,12] both in physiological and in pathological conditions. For example, LMP-dependent cell death is associated with mammary gland remodelling after weaning. In this model, Stat3 downregulation attenuates both LMP and cell death.[14] Although the molecular events that underlie LMP in the mammary gland remain unclear, the activation of Stat3 and calpain appears to have a prominent role.[14,39] Interestingly, Stat3 transcription is also upregulated and its phosphorylation increased in the rd10 retina at P20,[40] the time point at which we observed LMP in the present study. Moreover, this transcription factor is essential to determine photoreceptor cell fate during retinal development[41] and its cleavage has been linked to calpain activation.[42] Further experiments will thus be required to determine the role of Stat3 in LMP-dependent cell death in the retina.

There are multiple circumstances that can trigger LMP and cell death. Lysosomal membranes are protected by highly glycosylated proteins, which are highly susceptible to local oxidative attack. Lysosomes accumulate iron due to the continuous delivery of iron-containing proteins to the organelle. This increase in iron levels in turn favours the generation of the highly toxic hydroxyl radical through the Haber–Weiss reaction.[6] Several studies have demonstrated that iron chelation can attenuate reduced LMP and cell death *in vitro*.[43,44] Although the metallocomplex zinc-desferrioxamine ameliorates damage in the rd10 mouse retina,[45] it remains to be determined whether iron chelation can attenuate lysosomal-dependent cell death in this model.

Another strategy proven to protect against lysosomal-mediated cell death is overexpression of the chaperone Hsp70.[46] This chaperone stabilizes lysosomes by binding to endolysosomal lipids, thus enhancing the activity of acid sphingomyelinase, an important enzyme in sphingolipid catabolism. Interestingly, Nieman–Pick disease is caused by a mutation of this enzyme, and LMP precedes cell death and autophagy blockade in a mouse model of this disease as well as in fibroblasts from affected patients.[10] Photoreceptor cell death in an *in vivo* model of MNU toxicity is attenuated by valproic acid-induced increases in Hsp70 expression. Interestingly, in that same model, increased oxidative stress results in Hsp70 carbonylation and its subsequent degradation by calpain.[47] It has been recently proposed that a similar mechanism could contribute to the pathogenesis of other neurodegenerative diseases, such as Alzheimer's disease.[48] Calpain cleavage of other essential lysosomal proteins, such as Lamp-2, has also been recently reported.[49] It is thus tempting to speculate that similar degradation of essential lysosomal proteins could participate in lysosomal damage in rd10 retinas.

The role of autophagy in photoreceptor cells is only beginning to be understood. Recent reports have shown that suppression of autophagy *in vitro* protects photoreceptor cells from light-induced injury,[50] and that calpain inhibition restores autophagy after TNF-α-induced cell death.[36] In our retinal explant system, both *in vitro* and *in vivo*, we found that wortmannin attenuated cell death induced by calcium overload, whereas rapamycin and trehalose increased photoreceptor cell death. These data indicate that autophagy is detrimental in a system in which lysosomal function is impaired. In agreement with our observations, several studies have demonstrated that autophagy downregulation significantly attenuates LMP and neuronal cell death after lysosomal damage.[4,51] Similar observations have been reported in a model of cancer chemotherapy.[52] Our observations may also explain why autophagy downregulation exerts a protective effect in many models of ischaemic injury that are also associated with lysosomal alterations and LMP.[53,54]

As described in other models of retinitis pigmentosa,[55] we detected no caspase activation in rd10 retinas (data not shown). It has been recently suggested that dying photoreceptors in retinitis pigmentosa display features and kinetics that differ from those of classical apoptosis and necrosis and that may constitute a new type of cell death.[56] In some

degenerating photoreceptors in the rd10 retina, we detected DNA breaks associated with the lysosomal DNAse II that did not colocalize with the classical TUNEL-positive breaks. Further studies will be required to determine whether the lysosomal-induced cell death observed in this model represents a new, slower form of cell death.

In summary, we describe a sequence of events preceding photoreceptor cell death in a mouse model of retinitis pigmentosa that includes increased calcium levels, calpain activation, lysosomal damage, translocation of cathepsins to the cytosol. This lysosomal damage results in defects of autophagy that may be aggravated by an early block in autophagosome formation related to increased calpain activity. The identification of this pathway in the rd10 retina suggests that the calpain–cathepsin hypothesis, which has been associated with several other neurodegenerative conditions such as Alzheimer's disease and stroke, can also be applied to retinitis pigmentosa, and points to the possibility of common therapeutic strategies for these prevalent and incurable diseases.

Materials and Methods

Animal procedures. All procedures were approved by the respective local ethics committee for animal experimentation, and all experiments were carried out in accordance with the European Union guidelines and the ARVO Statement for the Use of Animals in Ophthalmic and Vision Research. Wt C57BL/6J mice and the rd10 mouse model of retinal degeneration, also on a C57BL/6J background and homozygous for the *Pde6* mutation, were obtained from The Jackson Laboratory (Bar Harbor, ME, USA). GFP-LC3 mice were kindly provided by Noboru Mizushima (Deparment of Physiology and Cell Biology at Tokyo Medical and Dental University, Tokyo, Japan).[57] Both male and female mice were used for this study and at least six animals per group were used. To avoid circadian variation in LC3 levels,[58] rd10 and Wt retinas were always dissected at the same time of the day: 1000 hours. For intravitreal injections, rd10 mice at P23 were undefined with isoflurane. By using a Hamilton syringe (Model 75 RN SYR) with 1-cm long 33- gauge removable needles, right eyes were intreavitreally injected with 1 μl of 80 μM ALLN or 1 μl of 400 μM leupeptin and 40 μg/ml pepstatin A, whereas the left eyes received 1 μl of the vehicle (0.4% DMSO in phosphate-buffered saline (PBS)). *In vivo* rapamycin treatments were performed as described previously[20] every 2 days in mice from P13. For intravitreal trehalose treatments, P19 mice were anesthetized with isoflurane, and right eyes were injected with 1 μl of 30 mM trehalose in PBS, whereas the left eyes received 1 μl of 30 mM sucrose in PBS. At the indicated ages, mice were killed and eyes fixed overnight with 4% PFA in 0.1 M phosphate buffer at 4 °C. Then, retinas were extracted and cell death detection was performed as described before.[59]

Immunostaining in retinal sections. Fixed eyes were washed with PBS and then cornea and lens were dissected. Optic cups were dehydrated with increasing sucrose concentrations (15–30% in PBS), embedded in Tissue-Tek (Sakura, Leiden, The Netherlands) and cut in a cryostat (Leica CM1850, Heerbrugg, Switzerland). Sections were then rehydrated, permeated with 0.5% Triton X-100 in PBS and incubated overnight at 4 °C with an antibody raised against Ambra1 in BGT, 0.3% BSA, 100 mM glycine and 0.25% Triton X-100 in PBS. Sections were then washed with PBS and incubated for 1 h with Alexa 546 (Invitrogen, Carlsbad, CA, USA), stained with DAPI (4',6-diamidino-2-phenylindole), mounted in DABCO and visualized using confocal microscopy.

Neuroretina organotypic culture. After enucleation of the eyes, all superfluous tissues were removed from the neuroretina, and then maintained in the chemically defined R16 medium[60] for the indicated times (between 1 and 24 h) at 37 °C in a 5% CO_2 atmosphere. Where indicated, retinas were incubated with 5 μM A23187, 10 μg/ml pepstatin A, 20 mM ammonium chloride (all from Sigma, St. Louis, MO, USA), 20 μM ALLN, 100 μM leupeptin, 100 nM rapamycin or 100 nM wortmannin (all from Calbiochem, Darmstadt, Germany). The retinas were then washed two times with PBS and flat-mounted into nitrocellulose membranes, fixed overnight in 4% paraformaldehyde (w/v) in 0.1 M phosphate buffer (pH 7.4) and processed. Cathepsin B activity was measured in neuroretinas using the Magic Red Cathepsin B Assay Kit (Immunochemistry Technologies, Bloomington, MN, USA) following the manufacturer's instructions, and then fixed with 4% PFA for 1 h, mounted into nitrocellulose filters, counterstained with DAPI and visualized by confocal microscopy.

Detection of cell death. Programmed cell death was visualized by TUNEL. Mice of the indicated genotype and age were killed, their eyes enucleated and the retinas removed and flat-mounted into nitrocellulose filters (Sartorius, Goettingen, Germany), with the photoreceptor layer facing up. Retinas were then fixed in 4% (w/v) paraformaldehyde in 0.1 M phosphate buffer (pH 7.4) at 4 °C overnight, permeated for 1 h at RT with 2% Triton X-100 (w/v; Fluka, St. Louis, MO, USA) in PBS, incubated with 20 μg/ml proteinase K (Sigma) for 10 min at 37 °C and subsequently processed for TUNEL staining following the manufacturer's instructions (Promega). After labelling, retinas were mounted with DABCO 4% (w/v; Sigma) and glycerol 70% (v/v) containing 1 μM DAPI and analysed on a confocal laser microscope (TCS SP5; Leica Microsystems, Wetzlar, Germany). Serial optical sections were acquired with a × 63 objective every 1 μm in four central fields around the optic nerve, avoiding the optic nerve head and the peripheral area. The ApopTag ISOL Dual Fluorescence Apoptosis Detection Kit (DNase Types I and II) (Millipore) was used following the manufacturer's instructions.

Staining of whole-mount retinas. Immunostaining was performed overnight at 4 °C using antibodies against Lamp-1 (Developmental Studies Hybridoma Bank), cathepsin B (Chemicon), Ambra1 (Covalab), N-tyr proteins (Millipore) or 8-OH deoxyguanosine (Millipore) after initial permeabilization with 2% Triton X-100 for 1 h at RT and subsequent incubation with the blocking solution (10% normal goat serum, 0.25% Triton X-100 in PBS). The retinas were then washed and incubated for 1 h with Alexa 546 or 488 (Invitrogen), stained with DAPI, mounted in DABCO and visualized using confocal microscopy.

Images obtained with a confocal microscope (TCS SP5; Leica Microsystems) as described above were further analysed for fluorescence intensity using Fiji software (Madison, WI, USA).[61] After subtracting backgrounds, histograms and mean intensities for CB, lamp1, N-tyr proteins or 8-OH deoxyguanosine, channels were quantified throughout the ONL. Ratio between CB and lamp1 fluorescence was calculated, and finally fluorescence means were statistically analysed with the GraphPad Prism 5 sofware (La Jolla, CA, USA).

Flow cytometry of dissociated retinas. Retinas were dissociated immediately after dissection, or after treatments, by incubating them in 1% (w/v) trypsin (Worthington, Lakewood, NJ, USA) in R16-defined medium for 5 min at 37 °C. Then, the retinas were dissociated by carefully pipetting them 12 times, and the enzyme activity was stopped by adding 10% FBS. The samples were then centrifuged at 1000 r.p.m. for 5 min at 20 °C, the supernatant removed and the dissociated tissue incubated with 1 μM Fluo-3AM (Invitrogen) to measure the calcium levels or with 10 μM DHE (Invitrogen) to analyse ROS levels in R16 medium for 30 min at 37 °C with 5% CO_2. Next, the dissociated retinas were resuspended in 300 μl of medium and then analysed in an XL flow cytometer (Beckman Coulter, Pasadena, CA, USA).

Western blot. Neuroretinas were lysed in a buffer containing 50 mM Tris-HCl (pH 6.8), 10% glycerol (v/v), 2% SDS (w/v), 10 mM DTT and 0.005% bromophenol blue. Fifteen micrograms of protein was resolved on 15% SDS-PAGE gel. The proteins were then transferred to PVDF membranes (Bio-Rad, Hercules, CA, USA), which were blocked for 1 h in PBS-Tween-20 (0.05% (v/v)) containing 5% non-fat milk and then probed with antibodies against LC3 (Sigma), p62 (Enzo, Farmingdale, NY, USA), P-S6, P-eIF2α and eIF2α (all from Cell Signaling, Danvers, MA, USA), calpain-1 (Calbiochem), calpain-2 (Sigma), recoverin, calpastatin and Beclin1 (all from Santa Cruz Biotechnology), tubulin (Sigma) or glyceraldehyde 3-phosphate dehydrogenase (GAPDH) (Abcam, Cambridge, MA, USA). The antibodies were detected using the appropriate horseradish peroxidase-labelled secondary antibodies (Pierce, Fife, WA, USA) and were visualized with the SuperSignal West Pico chemiluminescent substrate (Pierce). Densitometric analysis was performed with Quantity One software (Bio-Rad). When the protease inhibitors (N/L) were used, retinas were cut in two halves; culturing one *in contro* medium and the other one with a combination of 100 μM leupeptin (Thermo Fisher Scientific, Fife, WA, USA) and 20 mM ammonium chloride (Sigma) for 3 h before protein extraction.

Statistical analysis. Statistical analyses were performed with the GraphPad Prism 5 software. For flow cytometry measurement comparison, two-way ANOVA with Bonferroni posttest was used to compare Wt *versus* rd10 retinas. Student's *t*-test was used to analyse the results from the retinal explants, applying the Welch's correction when variances were significantly different. Results from the intreavitreal injections were analysed with the paired *t*-test, pairing each retina with its contralateral retina. In all the experiments, differences were considered significant when $P < 0.05$.

Conflict of Interest

The authors declare no conflict of interest.

Acknowledgements. This work was supported by grants from MINECO (Spain), SAF2012-36079 to PB, CONSOLIDER CSD2010-000454 to PB and EJdR and SAF2010-21879-C02-01 to EJdR. NRM was a recipient of a FPU fellowship from MICINN. We thank Dr. Teresa Suárez for her helpful comments and discussion and Maite Seisdedos for technical assistance.

1. Boya P, Reggiori F, Codogno P. Emerging regulation and functions of autophagy. *Nat Cell Biol* 2013; **15**: 713–720.
2. Schneider JL, Cuervo AM. Autophagy and human disease: emerging themes. *Curr Opin Genet Dev* 2014; **26C**: 16–23.
3. Harris H, Rubinsztein DC. Control of autophagy as a therapy for neurodegenerative disease. *Nat Rev Neurol* 2012; **8**: 108–117.
4. Nixon RA. The role of autophagy in neurodegenerative disease. *Nat Med* 2013; **19**: 983–997.
5. Cang C, Zhou Y, Navarro B, Seo YJ, Aranda K, Shi L *et al.* mTOR regulates lysosomal ATP-sensitive two-pore Na(+) channels to adapt to metabolic state. *Cell* 2013; **152**: 778–790.
6. Boya P. Lysosomal function and dysfunction: mechanism and disease. *Antioxid Redox Signal* 2012; **17**: 766–774.
7. Aits S, Jaattela M. Lysosomal cell death at a glance. *J Cell Sci* 2013; **126**: 1905–1912.
8. Lee JH, Yu WH, Kumar A, Lee S, Mohan PS, Peterhoff CM *et al.* Lysosomal proteolysis and autophagy require presenilin 1 and are disrupted by Alzheimer-related PS1 mutations. *Cell* 2010; **141**: 1146–1158.
9. Dehay B, Bove J, Rodriguez-Muela N, Perier C, Recasens A, Boya P *et al.* Pathogenic lysosomal depletion in Parkinson's disease. *J Neurosci* 2010; **30**: 12535–12544.
10. Gabande-Rodriguez E, Boya P, Labrador V, Dotti CG, Ledesma MD. High sphingomyelin levels induce lysosomal damage and autophagy dysfunction in Niemann Pick disease type A. *Cell Death Differ* 2014; **21**: 864–875.
11. Boya P, Andreau K, Poncet D, Zamzami N, Perfettini JL, Metivier D *et al.* Lysosomal membrane permeabilization induces cell death in a mitochondrion-dependent fashion. *J Exp Med* 2003; **197**: 1323–1334.
12. Boya P, Gonzalez-Polo RA, Poncet D, Andreau K, Vieira HL, Roumier T *et al.* Mitochondrial membrane permeabilization is a critical step of lysosome-initiated apoptosis induced by hydroxychloroquine. *Oncogene* 2003; **22**: 3927–3936.
13. Boya P, Kroemer G. Lysosomal membrane permeabilization in cell death. *Oncogene* 2008; **27**: 6434–6451.
14. Kreuzaler PA, Staniszewska AD, Li W, Omidvar N, Kedjouar B, Turkson J *et al.* Stat3 controls lysosomal-mediated cell death *in vivo*. *Nat Cell Biol* 2011; **13**: 303–309.
15. Vila M, Bove J, Dehay B, Rodriguez-Muela N, Boya P. Lysosomal membrane permeabilization in Parkinson disease. *Autophagy* 2011; **7**: 98–100.
16. Goll DE, Thompson VF, Li H, Wei W, Cong J. The calpain system. *Physiol Rev* 2003; **83**: 731–801.
17. Norman JM, Cohen GM, Bampton ET. The *in vitro* cleavage of the hAtg proteins by cell death proteases. *Autophagy* 2010; **6**: 1042–1056.
18. Sahara S, Yamashima T. Calpain-mediated Hsp70.1 cleavage in hippocampal CA1 neuronal death. *Biochem Biophys Res Commun* 2010; **393**: 806–811.
19. Rodriguez-Muela N, Koga H, Garcia-Ledo L, de la Villa P, de la Rosa EJ, Cuervo AM *et al.* Balance between autophagic pathways preserves retinal homeostasis. *Aging Cell* 2013; **12**: 478–488.
20. Rodriguez-Muela N, Germain F, Marino G, Fitze PS, Boya P. Autophagy promotes survival of retinal ganglion cells after optic nerve axotomy in mice. *Cell Death Differ* 2012; **19**: 162–169.
21. Porter K, Nallathambi J, Lin Y, Liton PB. Lysosomal basification and decreased autophagic flux in oxidatively stressed trabecular meshwork cells: implications for glaucoma pathogenesis. *Autophagy* 2013; **9**: 581–594.
22. Kim JY, Zhao H, Martinez J, Doggett TA, Kolesnikov AV, Tang PH *et al.* Noncanonical autophagy promotes the visual cycle. *Cell* 2013; **154**: 365–376.
23. Gargini C, Terzibasi E, Mazzoni F, Strettoi E. Retinal organization in the retinal degeneration 10 (rd10) mutant mouse: a morphological and ERG study. *J Comp Neurol* 2007; **500**: 222–238.
24. Barhoum R, Martinez-Navarrete G, Corrochano S, Germain F, Fernandez-Sanchez L, de la Rosa EJ *et al.* Functional and structural modifications during retinal degeneration in the rd10 mouse. *Neuroscience* 2008; **155**: 698–713.
25. Corrochano S, Barhoum R, Boya P, Arroba AI, Rodriguez-Muela N, Gomez-Vicente V *et al.* Attenuation of vision loss and delay in apoptosis of photoreceptors induced by proinsulin in a mouse model of retinitis pigmentosa. *Invest Ophthalmol Vis Sci* 2008; **49**: 4188–4194.
26. Sancho-Pelluz J, Arango-Gonzalez B, Kustermann S, Romero FJ, van Veen T, Zrenner E *et al.* Photoreceptor cell death mechanisms in inherited retinal degeneration. *Mol Neurobiol* 2008; **38**: 253–269.
27. Sarkar S, Davies JE, Huang Z, Tunnacliffe A, Rubinsztein DC. Trehalose, a novel mTOR-independent autophagy enhancer, accelerates the clearance of mutant huntingtin and alpha-synuclein. *J Biol Chem* 2007; **282**: 5641–5652.
28. Ureshino RP, Rocha KK, Lopes GS, Bincoletto C, Smaili SS. Calcium signaling alterations, oxidative stress, and autophagy in aging. *Antioxid Redox Signal* 2014; **21**: 123–137.
29. Paquet-Durand F, Beck S, Michalakis S, Goldmann T, Huber G, Muhlfriedel R *et al.* A key role for cyclic nucleotide gated (CNG) channels in cGMP-related retinitis pigmentosa. *Hum Mol Genet* 2011; **20**: 941–947.
30. Williams A, Sarkar S, Cuddon P, Ttofi EK, Saiki S, Siddiqi FH *et al.* Novel targets for Huntington's disease in an mTOR-independent autophagy pathway. *Nat Chem Biol* 2008; **4**: 295–305.
31. East DA, Campanella M. Ca^{2+} in quality control: an unresolved riddle critical to autophagy and mitophagy. *Autophagy* 2013; **9**: 1710–1719.
32. Hoyer-Hansen M, Bastholm L, Szyniarowski P, Campanella M, Szabadkai G, Farkas T *et al.* Control of macroautophagy by calcium, calmodulin-dependent kinase kinase-beta, and Bcl-2. *Mol Cell* 2007; **25**: 193–205.
33. Engedal N, Torgersen ML, Guldvik IJ, Barfeld SJ, Bakula D, Saetre F *et al.* Modulation of intracellular calcium homeostasis blocks autophagosome formation. *Autophagy* 2013; **9**: 1475–1490.
34. Xia HG, Zhang L, Chen G, Zhang T, Liu J, Jin M *et al.* Control of basal autophagy by calpain1 mediated cleavage of ATG5. *Autophagy* 2010; **6**: 61–66.
35. Kuro M, Yoshizawa K, Uehara N, Miki H, Takahashi K, Tsubura A. Calpain inhibition restores basal autophagy and suppresses MNU-induced photoreceptor cell death in mice. *In Vivo* 2011; **25**: 617–623.
36. Chinskey ND, Zheng QD, Zacks DN. Control of photoreceptor autophagy after retinal detachment: the switch from survival to death. *Invest Ophthalmol Vis Sci* 2014; **55**: 688–695.
37. Pagliarini V, Wirawan E, Romagnoli A, Ciccosanti F, Lisi G, Lippens S *et al.* Proteolysis of Ambra1 during apoptosis has a role in the inhibition of the autophagic pro-survival response. *Cell Death Differ* 2012; **19**: 1495–1504.
38. Wang Y, Shen J, Xiong X, Xu Y, Zhang H, Huang C *et al.* Remote ischemic preconditioning protects against liver ischemia–reperfusion injury via heme oxygenase-1-induced autophagy. *PloS one* 2014; **9**: e98834.
39. Arnandis T, Ferrer-Vicens I, Garcia-Trevijano ER, Miralles VJ, Garcia C, Torres L *et al.* Calpains mediate epithelial-cell death during mammary gland involution: mitochondria and lysosomal destabilization. *Cell Death Differ* 2012; **19**: 1536–1548.
40. Samardzija M, Wariwoda H, Imsand C, Huber P, Heynen SR, Gubler A *et al.* Activation of survival pathways in the degenerating retina of rd10 mice. *Exp Eye Res* 2012; **99**: 17–26.
41. Pinzon-Guzman C, Zhang SS, Barnstable CJ. Specific protein kinase C isoforms are required for rod photoreceptor differentiation. *J Neurosci* 2011; **31**: 18606–18617.
42. Oda A, Wakao H, Fujita H. Calpain is a signal transducer and activator of transcription (STAT) 3 and STAT5 protease. *Blood* 2002; **99**: 1850–1852.
43. Castino R, Bellio N, Nicotra G, Follo C, Trincheri NF, Isidoro C. Cathepsin D-Bax death pathway in oxidative stressed neuroblastoma cells. *Free Radic Biol Med* 2007; **42**: 1305–1316.
44. Eno CO, Zhao G, Venkatanarayan A, Wang B, Flores ER, Li C. Noxa couples lysosomal membrane permeabilization and apoptosis during oxidative stress. *Free Radic Biol Med* 2013; **65**: 26–37.
45. Obolensky A, Berenshtein E, Lederman M, Bulvik B, Alper-Pinus R, Yaul R *et al.* Zinc-desferrioxamine attenuates retinal degeneration in the rd10 mouse model of retinitis pigmentosa. *Free Radic Biol Med* 2011; **51**: 1482–1491.
46. Kirkegaard T, Roth AG, Petersen NH, Mahalka AK, Olsen OD, Moilanen I *et al.* Hsp70 stabilizes lysosomes and reverts Niemann–Pick disease-associated lysosomal pathology. *Nature* 2010; **463**: 549–553.
47. Koriyama Y, Sugitani K, Ogai K, Kato S. Heat shock protein 70 induction by valproic acid delays photoreceptor cell death by *N*-methyl-*N*-nitrosourea in mice. *J Neurochem* 2014; **130**: 707–719.
48. Yamashima T. Reconsider Alzheimer's disease by the 'calpain-cathepsin hypothesis'—a perspective review. *Prog Neurobiol* 2013; **105**: 1–23.
49. Villalpando Rodriguez GE, Torriglia A. Calpain 1 induce lysosomal permeabilization by cleavage of lysosomal associated membrane protein 2. *Biochim Biophys Acta* 2013; **1833**: 2244–2253.
50. Zhang TZ, Fan B, Chen X, Xu WJ, Jiao YY, Su GF *et al.* Suppressing autophagy protects photoreceptor cells from light-induced injury. *Biochem Biophys Res Commun* 2014; **450**: 966–972.
51. Walls KC, Ghosh AP, Franklin AV, Klocke BJ, Ballestas M, Shacka JJ *et al.* Lysosome dysfunction triggers Atg7-dependent neural apoptosis. *J Biol Chem* 2010; **285**: 10497–10507.

52. Gonzalez P, Mader I, Tchoghandjian A, Enzenmuller S, Cristofanon S, Basit F *et al.* Impairment of lysosomal integrity by B10, a glycosylated derivative of betulinic acid, leads to lysosomal cell death and converts autophagy into a detrimental process. *Cell Death Differ* 2012; **19**: 1337–1346.
53. Lipton P. Lysosomal membrane permeabilization as a key player in brain ischemic cell death: a 'lysosomocentric' hypothesis for ischemic brain damage. *Transl Stroke Res* 2013; **4**: 672–684.
54. Ginet V, Spiehlmann A, Rummel C, Rudinskiy N, Grishchuk Y, Luthi-Carter R *et al.* Involvement of autophagy in hypoxic–excitotoxic neuronal death. *Autophagy* 2014; **10**: 846–860.
55. Doonan F, Donovan M, Cotter TG. Caspase-independent photoreceptor apoptosis in mouse models of retinal degeneration. *J Neurosci* 2003; **23**: 5723–5731.
56. Sahaboglu A, Paquet-Durand O, Dietter J, Dengler K, Bernhard-Kurz S, Ekstrom PA *et al.* Retinitis pigmentosa: rapid neurodegeneration is governed by slow cell death mechanisms. *Cell Death Dis* 2013; **4**: e488.
57. Mizushima N, Yamamoto A, Matsui M, Yoshimori T, Ohsumi Y. *In vivo* analysis of autophagy in response to nutrient starvation using transgenic mice expressing a fluorescent autophagosome marker. *Mol Biol Cell* 2004; **15**: 1101–1111.
58. Yao J, Jia L, Shelby SJ, Ganios AM, Feathers K, Thompson DA *et al.* Circadian and noncircadian modulation of autophagy in photoreceptors and retinal pigment epithelium. *Invest Ophthalmol Vis Sci* 2014; **55**: 3237–3246.
59. Mellén MA, de la Rosa EJ, Boya P. The autophagic machinery is necessary for removal of cell corpses from the developing retinal neuroepithelium. *Cell Death Differ* 2008; **15**: 1279–1290.
60. Caffe AR, Ahuja P, Holmqvist B, Azadi S, Forsell J, Holmqvist I *et al.* Mouse retina explants after long-term culture in serum free medium. *J Chem Neuroanat* 2001; **22**: 263–273.
61. Schindelin J, Arganda-Carreras I, Frise E, Kaynig V, Longair M, Pietzsch T *et al.* Fiji: an open-source platform for biological-image analysis. *Nat Methods* 2012; **9**: 676–682.

Supplementary Information accompanies this paper on Cell Death and Differentiation website (http://www.nature.com/cdd)